High-Resolution 3D Multimodality Imaging to Resolve Intramural Human Sinoatrial Node Pacemakers and Epi-Endocardial Atrial Exit Sites

Ning Li, MD, PhD[1,2], **Brian J. Hansen, MD, PhD**[1,2], **James Kennelly**[6], **Anuradha Kalyanasundaram, PhD**[1,2], **Adel Kanaan**[1,2], **Orlando P. Simonetti, MD**[3,4], **Peter J. Mohler, PhD**[1,2], **Bryan Whitson, MD**[5], **John D. Hummel, MD**[2,3], **Jichao Zhao, PhD**[6], **Vadim V. Fedorov, PhD**[1,2]

[1]Department of Physiology & Cell Biology The Ohio State University Wexner Medical Center, Columbus, OH

[2]Bob and Corrine Frick Center for Heart Failure and Arrhythmia The Ohio State University Wexner Medical Center, Columbus, OH

[3]Division of Cardiovascular Medicine The Ohio State University Wexner Medical Center, Columbus, OH

[4]Department of Radiology The Ohio State University Wexner Medical Center, Columbus, OH

[5]Division of Cardiac Surgery, The Ohio State University Wexner Medical Center, Columbus, OH

[6]Auckland Bioengineering Institute, The University of Auckland; Auckland, New Zealand

Keywords

sinoatrial node; crista terminalis; optical mapping; magnetic resonance imaging

The human sinoatrial node (SAN) is an elongated 3D fibrotic structure located intramurally along crista terminalis (CT)[1]. During sinus rhythm, electrical activation originates from the intramural SAN pacemakers and conducts through the sinoatrial conduction pathways, which may lead to widely distributed epicardial (Epi) and endocardial (Endo) early activation exit sites along CT[2]. Surgical and ablation treatments for SAN and atrial arrhythmias may either target or preserve the SAN[1]. However, in the clinical setting, defining the intramural SAN pacemaker (Figure A) is challenging since electrode mapping defines only Epi and/or Endo surface conduction exits from the SAN[3, 4]. We hypothesize that human SAN pacemakers have distinct structural signatures that are different from Epi and Endo exit sites.

Correspondence: Vadim V. Fedorov, PhD, Department of Physiology and Cell Biology, The Ohio State University Wexner Medical Center, 5196 Graves Hall, 333 W 10th Ave. Columbus, OH 43210-1218, Tel: 1-614-366-0986, Fax: 1-614-292-4888, vadim.fedorov@osumc.edu.

To resolve the transmural structural signatures of human SAN-pacemaker-conduction complex, we developed a computational 3D imaging approach based on integrated high-resolution dual-sided near-infrared optical mapping (NIOM, 330–450μm^2) and contrast-enhanced magnetic resonance imaging (CE-MRI, 80–100μm^3). The Institutional review board defined the study on samples from deceased donors as Not Human Subjects Research. The data and methods are available from the corresponding author upon request.

Simultaneous sub-Epi/sub-Endo NIOM was conducted on coronary-perfused SAN-atria preparations isolated from cardioplegically-arrested non-failing donor hearts without arrhythmia history (n=4, 47±16y.o.). SAN pacemakers were identified by slow upstroke of optical action potentials preceding fast atrial upstrokes (Figure C). SAN pathways were identified as the preferential conduction path between the SAN and the earliest exit sites[2]. Physiological challenges[2] with adenosine (10μM) and/or 2Hz-3.3Hz atrial pacing were used to unmask additional Epi-Endo exits along with baseline exits for following structural analysis[2, 5]. Figure A shows the CE-MRI section across intramural SAN pacemaker with measurements of mapped SAN structures. Based on these measurements, we segmented 3D CE-MRI of the mapped SAN-atrial regions into 24×24 grids (~1.3–1.5mm^2, X-Y) and sub-Epi, intramural, and sub-Endo layers (25%, 50% and 25% of the wall thickness, respectively), for region-specific (SAN pacemakers vs exits) quantitative analysis of 3D myofiber orientation, fibrotic content, and wall thickness. Figure B shows 3D CE-MRI of SAN #1 superimposed with NIOM-defined SAN pacemakers and exits on wall thickness map.

All ex-vivo preparations had stable sinus rhythm (n=4, 74±12 bpm) at baseline with pacemakers in the SAN center. Figure C shows an example of slow conduction from the intramural SAN pacemaker through the lateral conduction pathway to earliest Epi exit followed by two Endo exits. Myofibers across the SAN (Figure D, Z-Y Section **1**) were predominantly oriented parallel to Epi-Endo surfaces. In contrast, CT (Z-Y Section **2**) had myofibers with transmural orientations (perpendicular to Epi-Endo surface) that might facilitate conduction emerging at Epi and Endo exit sites. Furthermore, intramural myofibers (Figure E, X-Y plane) of the conduction pathway had preferential orientation from the SAN pacemaker towards the earliest Epi exit, where they merged with CT myofibers. From Epi and Endo exit sites, preferential myofiber orientations supported faster conduction along CT through Endo vs Epi layers, leading to Epi-Endo activation delay variations from +11ms to −8ms along CT.

In total 20 recordings (~5/heart), SAN conduction exited primarily through lateral superior-inferior conduction pathways, which led to majority of Epi or Endo earliest exits (85%) were distributed on the CT. NIOM detected unicentric earliest exits on the Epi (n=7) or Endo (n=13) with subsequent (after 4.6±3.1ms) unicentric (n=8) or multicentric (n=12) secondary exits on the other atrial surface. Epi-Endo activation delay measured at the earliest exit sites varied along the superior (16.8±9.8ms, n=4), middle (8.3±2.5ms, n=8), inferior CT (9.4 ±3.7ms, n=5) and septal regions (9.3±5.7ms, n=3). Quantitative analysis of 3D structural features showed that (1) local transmural myofiber angles were larger within SAN pacemaker regions than exit sites (37.6±11.9° vs 22.4±14.4°, *p*=0.001, Figure F); (2) intramural and sub-Endo fibrotic contents were significantly higher within SAN pacemakers

than exits (45.7±10.9% vs 27.7±16.3%, *p*<0.001, and 40.7±14.8% vs 28.0±16.0%, *p*=0.009, Figure G); (3) wall thickness was significantly less across the SAN pacemakers than exits(3.7±1.1mm vs 5.2±2.mm, *p*=0.02, Figure B, **right**). Two tailed Mann-Whitney test were used.

In summary, we report the new quantitative 3D imaging approach that revealed the SAN leading pacemaker sites have significantly different structural features compared to Epi and Endo exits. Fibrotic insulation and transversal uncoupling of intramural SAN myofibers from Epi and Endo layers, together with preferential myofiber orientation from intramural SAN toward CT, provide mechanistic rational for the distant (4–23 mm from SAN) Epi and Endo exits primarily along thick CT but not directly on the SAN Epi or Endo surface projections. The early atrial exit sites can be distinguished from SAN pacemakers by region-specific transmural myofiber orientation, intramural and sub-Endo fibrotic content, and wall thickness. Further studies are warranted to confirm our findings in larger cohorts, including hearts with structural fibrotic remodeling and arrhythmia history. The developed 3D approach can help during clinical electrode mapping to guide patient-specific targeted ablation of the SAN and atrial arrhythmias.

Acknowledgments:

Sources of Funding:

Nonstandard Abbreviations and Acronyms

CE-MRI	contrast-enhanced magnetic resonance imaging
CT	crista terminalis
Epi	epicardial
Endo	endocardial
NIOM	near-infrared optical mappi
SAN	sinoatrial node

References:

1. Kalyanasundaram A, Li N, Augostini RS, Weiss R, Hummel JD, Fedorov VV. Three-Dimensional Functional Anatomy of Human Sinoatrial node for Epicardial and Endocardial Mapping and Ablation. Heart Rhythm. 2023;1:122–133.

2. Li N, Hansen BJ, Csepe TA, Zhao J, Ignozzi AJ, Sul LV, Zakharkin SO, Kalyanasundaram A, Davis JP, Biesiadecki BJ, et al. Redundant and diverse intranodal pacemakers and conduction pathways protect the human sinoatrial node from failure. Sci Transl Med. 2017;9:eaam5607.

3. Kharbanda RK, Wesselius FJ, van Schie MS, Taverne Y, Bogers A, de Groot NMS. Endo-Epicardial Mapping of In Vivo Human Sinoatrial Node Activity. JACC Clin Electrophysiol. 2021;6:693–702.

4. Parameswaran R, Lee G, Morris GM, Royse A, Goldblatt J, Larobina M, Watts T, Nalliah CJ, Wong G, Al-Kaisey AM, et al. Simultaneous epicardial-endocardial mapping of the sinus node in humans with structural heart disease: Impact of overdrive suppression on sinoatrial exits. Heart Rhythm. 2020;17:2154–2163. [PubMed: 32622994]

5. Csepe TA, Zhao J, Sul LV, Wang Y, Hansen BJ, Li N, Ignozzi AJ, Bratasz A, Powell KA, Kilic A, et al. Novel application of 3D contrast-enhanced CMR to define fibrotic structure of the human sinoatrial node in vivo. Eur Heart J Cardiovasc Imaging. 2017;18:862–869. [PubMed: 28087602]
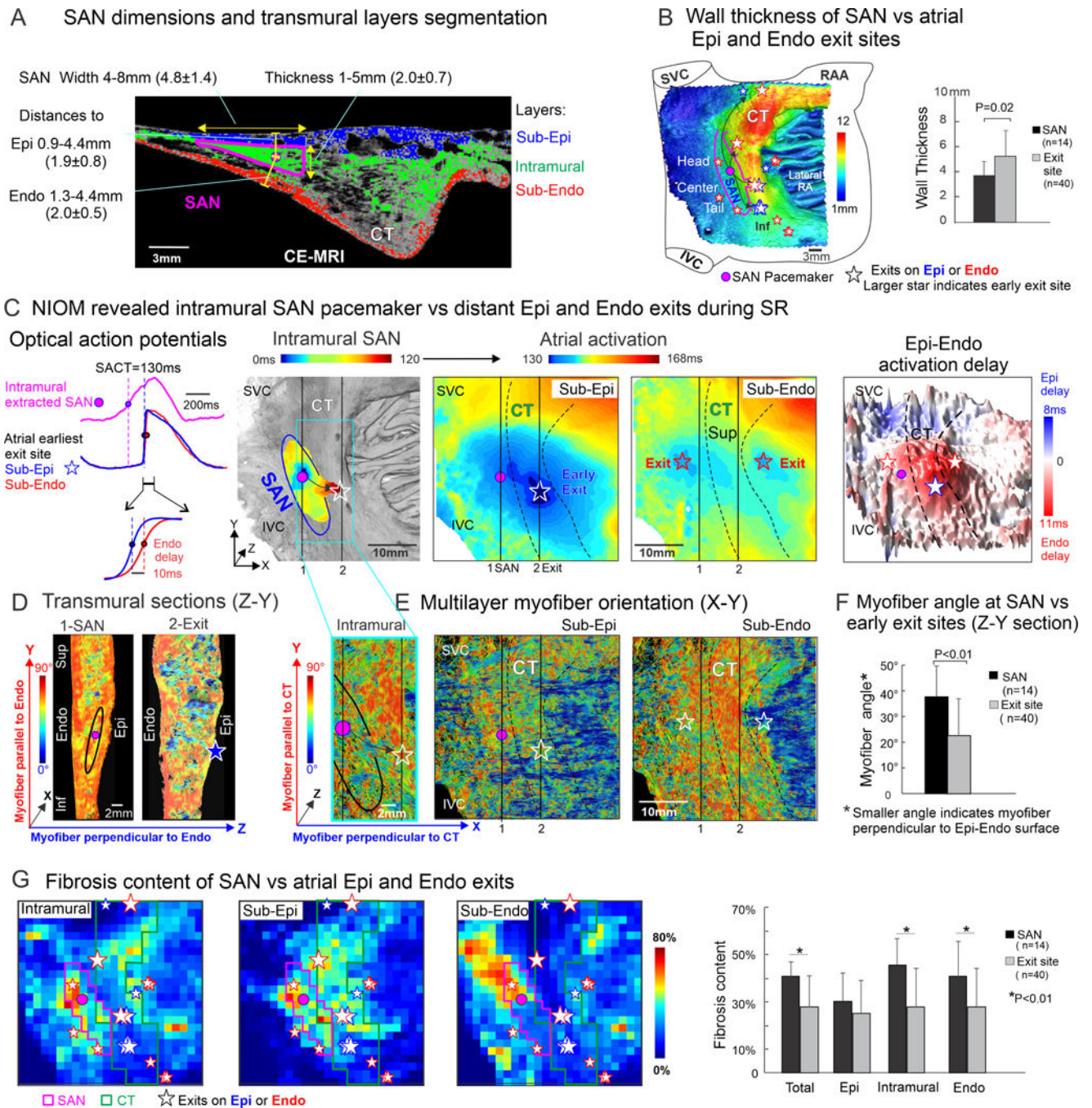
Figure.

Three-dimensional functional-structural architecture of human sinoatrial node and Epi-Endocardial atrial ehxit sites. **A**. SAN pacemaker tissue width, thickness and intramurality (distance to Epi and Endo) measurements (n=136 measurements from 4 hearts) shown on representative CE-MRI 2D section (resolution 100μm^3, Siemens HealthCare, SAN #1). Atrial wall was segmented into Sub-Epi (blue), intramural (green) and Sub-Endo (red) layers for quantitative structural analysis. **B**, Left, 3D CE-MRI of SAN #1 (66 y.o. male) with superimposed SAN pacemakers and exits (summary of SAN exit patterns during baseline,

adenosine and post atrial pacing). Larger stars filled with grey color indicate early exit sites. Wall thickness showed in color scale. Right, comparison of wall thickness at SAN pacemakers vs atrial exit sites (n= pacemaker or exit sites for analysis, N=3 hearts). **C**, Left, optical action potentials from SAN #1 pacemaker and Sub-Epi vs Sub-Endo atria of earliest atrial exit site. Middle, NIOM activation maps of intramural SAN and simultaneous sub-Epi and sub-Endo atria (with near-infrared dye di-4-ANBDQBS; and CMOS camera, MiCAM Ultima-L, SciMedia) revealed intramural SAN activation conduction from the leading pacemaker through lateral middle preferential conduction pathway to an unicentric earliest exit on Epi (blue star) and multicentric exits (two red stars) on Endo during baseline sinus rhythm. Right, 3D Epi-Endo transmural activation delay map showed Epi delay in blue color and Endo delay in red color. The Epi-Endo delay at the earliest exit site (blue star) was 10ms. **D**, Transmural myofiber orientations (SAN #1, Z-Y plane) on sections across the SAN pacemaker (section 1) and CT early exit site (section 2). Z axis- transmural direction, perpendicular to Endo. Y axis- longitudinal superior-inferior direction, along CT. Blue color indicates myofiber perpendicular to Endo (Z direction). Red color indicates myofiber parallel to Endo (Y directions). **E**, Multilayer myofiber orientation (X-Y plane) at intramural SAN pacemaker layer, and atrial Sub-Epi and Sub-Endo exits layers. X axis -transversal lateral direction, perpendicular to CT; Y axis- longitudinal superior-inferior direction, alone CT. Blue and red color indicate myofiber perpendicular (X direction) or parallel to CT (Y-direction). The pink dot indicates SAN pacemaker. Stars indicate Epi and Endo exits. Line 1 &2 indicate locations of transmural sections. **F,** Myofiber angle on Z-Y sections. Smaller myofiber angle indicates transmural myofiber perpendicular to Epi-Endo surface (n= pacemaker or exit sites for analysis, N=3 hearts). **G**, Left, Grid plot of CE-MRI multilayer fibrosis content of SAN-CT region (SAN #1); Right, comparison of fibrosis content at SAN pacemaker location vs atrial exit sites (n= pacemaker or exit sites for analysis, N=3 hearts). All Data are presented as means ± SD. Statistical analyses were performed in GraphPad Prism 8.0. Normality was tested using Kolmogorov-Smirnov test. Comparisons of SAN vs exits structural features were done using 2-tailed Mann Whitney test, and p-values <0.05 were considered significant. Abbreviations: CE-MRI, contrast-enhanced magnetic resonance imaging; CT, crista terminalis; Epi-Endo, epicardial-endocardial; Inf/Sup, inferior/superior; IVC/SVC, inferior/superior vena cava; NIOM, near-infrared optical mapping; RAA, right atrial appendage; SACT, sinoatrial conduction time; SAN, sinoatrial node.